submitted Dec 16, 02

Potential Dependence of the Step Line Tension on Surfaces in Contact with an Electrolyte

Harald Ibach and Margret Giesen

Institut für Schichten und Grenzflächen, ISG3, Forschungszentrum Jülich,

52425 Jülich, Germany

Wolfgang Schmickler

Abteilung Elektrochemie, Universität Ulm 89069 Ulm, Germany

Keywords: single crystal electrode, capacitance, double layer, interfacial structure, tension, theory

Abstract

The potential dependence of the step line tension for electrodes in contact with an electrolyte, but without specific adsorption, is calculated by solving the Poisson-Boltzmann equation numerically. Two contributions to the potential dependence are found. A contribution arising from the step geometry is zero at pzc and positive for either sign of the potential. The prevailing contribution arises from the dipole moment of the charge distribution at steps. It is approximately proportional to the dipole moment and the specific surface charge, and negative for potentials positive of pzc.

Corresponding author: Harald Ibach, Research Center Jülich, ISG3, 52425 Jülich Germany

e-mail: h.ibach@fz-juelich.de, Tel. (+49) 2461 614561 FAX (+49) 2461 613907

Introduction

Due to the growing interest in the generation and functionalization of nano-scale structures on solid templates considerable attention has been devoted lately to the energetics and dynamics of monatomic steps on single crystal surface, be it on surfaces in vacuum or on surfaces in contact with an electrolyte [1, 2]. For the purpose of quantitative studies two types of idealized step structures are particular suitable: Extended straight steps, ideally infinitely long, as they exist on vicinal surfaces and closed loops of steps such as provided by two-dimensional islands of monatomic height. In both cases the individual steps may be in quasi-equilibrium with other steps and the rest of the surface. On a vicinal surface, e. g., repulsive interactions (entropy and elastic energy) stabilize the position of a step to remain near the mean step-step distance, and the step position fluctuates around that mean position. The closed step along the perimeter of an island is also frequently in a quasi equilibrium state insofar as the diffusion along the perimeter of an island is typically much faster than the attachment and detachment processes which are the time limiting steps involved in inter-island and interlayer mass transport. On a solid surface, and in particular on metal surfaces, the step which defines an individual island is in equilibrium with itself. A uniform chemical potential may therefore be attributed to the entire perimeter of an island. Because of these quasi-equilibrium situations and the small spatial and time gradients in the chemical potential, the energetics and dynamics of steps on a mesoscopic scale can be described in terms of thermodynamics with thermodynamic functions varying slowly in space and time. By using this thermodynamic approach methods have been developed lately which enable the determination of the step line tension from island equilibrium shapes [3, 4] and island shape fluctuations [5, 6]. Whereas these methods were originally developed for surfaces in vacuum, they can likewise be applied to surfaces in contact with an electrolyte [7-9]. In the latter case, the interfacial Gibbs free energy associated with a step (henceforth called the line tension of a step) is determined for which the electrode potential is the independent variable. We note that this is a different thermodynamic quantity than considered and measured in vacuum surface physics. There, one considers and measures the Helmholtz step free energy per length for which the step charge is the independent variable (confusingly also called "line tension"). The most remarkable aspect of the studies of [7-9] is the strong dependence of the line tension of steps on the Au(100) surface in contact with 50 mM H_2SO_4 on the electrode potential. The work presented with this paper was largely inspired by these results. As a first step towards an understanding of the observed potential dependence of the line tension we intend to explore the contribution of the outer space charge layer of ions in the electrolyte on the line tension, while the effect of a modification at steps with respect to the inner Helmholtz-layer, the electronic response of the metal and specific adsorption is left to future studies. The outer space charge layer in the electrolyte contributes to the line tension of a step for two entirely different reasons. One reason is that the step represents a particular type of surface roughness which changes (reduces, as we shall see) the interfacial capacitance near a step. A second contribution arises from the local potential at a step owed to the Smoluchowski-effect [10]. The far field of this potential can be described by a step dipole moment. The perpendicular component of this dipole moment gives rise to the observed reduction in the work function of stepped surfaces [11, 12] and to a shift in the potential of zero charge (pzc) [13, 14]. The effect of the roughness and the potential on the line tension are studied (i) by solving the Poisson-Boltzmann equation for the space charge layer of ions in the electrolyte numerically and (ii) with the help of simple semi-quantitative analytical models. In the present approach, the potential distribution at a step will be modeled by the potential of a point dipole. In a future study the potential distribution and its effect on the potential dependence of the step line tension will be calculated using pseudo-potentials [15].

The key result of this paper is that indeed the space charge layer adds a considerable, potential dependent contribution to the line tension which is of the same order of magnitude as the experimentally observed effect. It will be shown furthermore that to a good approximation the potential dependence of the line tension can be expressed in terms of the shift in the pzc on stepped surfaces and the potential dependence of the surface charge.

The paper is organized as follows. In the following section the line tension of a step on an electrode which is in equilibrium with an electrolyte is defined, and the relation to the step capacitance is established. In section 3 analytically solvable models for the step capacitance and the step tension are presented. Section 4 describes the model which is used for the step geometry and the electric properties of a step, and the method for the numerical solution of the Poisson-Boltzmann equation is elucidated. The results of the simulations are presented in section 5 and discussed in connection with the analytical models.

2. The line tension of a step in equilibrium with an electrolyte

The line tension of a step (denoted as β) on a surface which is in equilibrium with an electrolyte can be defined analog to the surface tension γ. We note again that this surface tension differs from the surface tension as normally defined in surface physics, where it is the Helmhotz free energy per area $g^{(H)}$, while here the surface tension is the Gibbs free energy per area $g^{(G)}$ for which the electrode potential is the independent variable. The two surface tensions are related by the Lagrange transformation

$$g^{(G)} = g^{(H)} - fs - \sum_i m_i G_i \qquad (1)$$

Here s and f are the surface charge density on the metal and the potential, and G_i and m_i are the surface excess and the chemical potential of all solution species except the solvent, respectively. Since we are interested in the potential dependence of the line tension rather than in an absolute value we use the differential formulation of the electrocapillary equation for the surface tension ($g^{(G)}$, from now on simply denoted as g) as the starting point [16, 17]:

$$dg \quad = -s d f - \sum_i G_i dm_i \tag{2}$$

We assume that the surface has a single straight step that extends along the cartesian coordinate y at x = 0. In other words, the surface is now defined by contour function z(x) with the limiting values $\lim_{x \to -\infty} z(x) = h$ and $\lim_{x \to +\infty} z(x) = 0$, with h the step height. The presence of the step modifies the surface charge density and the surface excess near the step position. Consequently, the charge density and the surface excess become a function of x, and so does the surface tension g. The line tension to be attributed to the step is therefore the difference between the surface tension of a surface with the step g_s(x) and the surface without the step g_0, integrated over the coordinate x perpendicular to the step direction. We can therefore write for the differential line tension db:

$$\mathrm{d}b = \lim_{L \to \infty} \int_{-L}^{L} \mathrm{dx}(dg_s(\mathrm{x}) - dg_0) \tag{3}$$

and hence

$$\mathrm{d}b = -\lim_{L \to \infty} \int_{-L}^{L} \mathrm{dx}\left[\left(s_s(\mathrm{x}) - s_0\right) d f + \sum_i \left(G_{i,s}(\mathrm{x}) - G_{i,0}\right) dm_i \right]. \tag{4}$$

The indices s and 0 denote quantities on a surface with and without a step, respectively. The integration range L must be sufficiently large so that $s_s(\pm L) = s_0$ and $G_{i,s}(\pm L) = G_{i,0}$. Because of the integration along the x-axis the line tension b is an energy per length rather than per area, as it should be. We remark that in an entirely numerical calculation the line tension can be calculated as difference in the total Gibbs free energy of a surface with and without a step divided by the step length. Hence no explicit integration is needed in that case. The form of eqs. 3/4 however lends itself to analytical model calculations, as will be shown in the following. In principle, eq. (4) could be used as a basis for a step chronocoulometry in a similar way as eq. (2) is employed for the chronocoulometry of a surface [18, 19]. The method would require the possibility of measuring a step charge. While no direct method for the determination of a step charge on a single step seems at hand (see however [12]) the step charge density could be measured as the difference of the surface charges on a vicinal crystal with regular step arrays and a flat surface of the same area. In the following we focus on the contribution of the first term in eq. (4) to the line tension that arises from the excess charge at the step, while any excess adsorption at the step is neglected.

A differential step capacitance can be defined following the procedure as described above:

$$C_{step}(f) = \lim_{L\to\infty} \int_{-L}^{L} \mathrm{dx} \left(\frac{\partial s_s(\mathrm{x})}{\partial f} - \frac{\partial s_0}{\partial f} \right) \qquad (5)$$

Again, the step capacitance C_{step} is a capacitance per length along the step direction. The line tension b can be calculated from the step capacitance simply by integration at constant chemical potential μ_i in a similar way as the surface tension is calculated from the surface capacitance using the Lippmann equation (see e. g. [16]). Our task to calculate the potential dependence of the line tension thus reduces to a calculation of the step capacitance as a function of the electrode potential.

3. Analytically solvable models

The potential f(x,y,z) in the space charge layer of the electrolyte near a charged metal electrode is described by a self-consistent solution of the Poisson-equation together with Boltzmann statistics for the concentration of ions in the electrolyte. We assume a neutral electrolyte with concentration n_0 of ions, with positive and negative ions having the same valence Z. The charge density ρ(x,y,z) is then

$$\rho(x,y,z) = Zn_0\left(e^{\frac{eZ\varphi(x,y,z)}{k_BT}} - e^{-\frac{eZ\varphi(x,y,z)}{k_BT}}\right). \tag{6}$$

The reference level φ(x,y,z) = 0 is the neutral electrolyte. The charge density ρ(x,y,z) and the potential φ(x,y,z) also obey the Poisson-equation

$$\Delta\varphi(x,y,z) = \frac{\rho(x,y,z)}{\varepsilon\varepsilon_0} \tag{7}$$

in which ε and ε_0 are the relative and the vacuum permittivities, respectively. Eqs.(6) and (7) can be solved analytically for the one-dimensional case (Gouy-Chapman theory) [16, 20, 21]. Assuming that the metal surface is the x,y plane the potential φ(z) is

$$\varphi(z) = \frac{4k_BT}{Ze}\arctan\left\{e^{-\kappa z}\tanh\left(\frac{Ze\varphi_G}{4k_BT}\right)\right\} \tag{8}$$

where κ^{-1} is the Debye length

$$d_{Debye} = \kappa^{-1} = \left(\frac{\varepsilon\varepsilon_0 k_BT}{2Z^2 n_0 e^2}\right)^{1/2} \tag{9}$$

and φ_G denotes the potential at a boundary between the layer of immobilized species at the electrode and the liquid electrolyte with mobile ions. The charge density at this boundary σ_G is

$$\sigma_G = \frac{2\varepsilon\varepsilon_0\kappa k_BT}{Ze}\sinh(Ze\varphi_G/2k_BT) \tag{10}$$

The capacitance (per surface area) of the space charge region of mobile ions C_G (Gouy-Chapman capacitance) is

$$C_G = \frac{\partial\sigma_G}{\partial\varphi_G} = \varepsilon\varepsilon_0\kappa\cosh(Ze\varphi_G/2k_BT) \tag{11}$$

The capacitance has a minimum at the potential of zero charge (pzc) $\varphi_G = 0$ which is

$$C_G = \varepsilon\varepsilon_0\kappa\,. \tag{12}$$

The Gouy-Chapman theory does not take into account the finite size of the ion cores and the repulsive interactions between the ions. As a consequence, the surface charge becomes unrealistically large for larger deviation from pzc. In order to correct for this deficiency the Gouy-Chapmann capacitance can be considered as being in series with an additional Helmholz-capacitance C_H which is of the order of 20-100 μF/cm^2 and a slower varying function of the electrode potential so that the total capacitance becomes

$$C_{tot}^{-1} = C_H^{-1} + C_G^{-1} . \tag{13}$$

For lower concentrations of the electrolyte $C_G < C_H$ near pzc, $\phi_0 = 0$, the total capacitance is mainly determined by the Gouy-Chapman capacitance C_G. The same holds for the potential dependence of the total capacitance. The original rational for introducing the Helmholtz-capacitance was the assumption of a Stern-layer of immobile water molecules at the surface. As shown by Schmickler and Henderson [22] more realistic models which include finite size effects for the ions and the dielectric response of the metal surface can also be cast into the form of a Helmholtz-capacitance C_H in series with the Gouy-Chapman capacitance.

The capacitance of a surface with a step can be calculated by solving the Poisson-Boltzmann equation numerically with the boundary conditions set by the geometrical structure and the surface potential of the step. The numerical solution will be considered in the next section. In the remainder of this section we consider the effect of the new boundary conditions qualitatively and present an approximate analytical expression in certain limits for the step capacitance and the step tension. In the absence of any better knowledge, the Helmholtz-capacitance at the step and the thickness of the layer of immobile ions at the surface are assumed to be independent of the surface potential and to be the same as on the flat surface. While this assumption is certainly not justified it is a reasonable approach for potentials near pzc and for electrolytes of low concentration because of the small contribution of the Helmholtz-capacitance to the total capacitance.

The influence of the step geometry on the capacitance can be qualitatively understood by considering the equi-potential lines in the space layer of ions (Fig. 1). At the distance d_{Debye} where, according to the Gouy-Chapman theory the effective counter electrode resides, the equi-potential contour follows the step contour but smoothly over a lateral distance which is approximately again the screening length d_{Debye}. This leads to an effective reduction of the surface capacitance in a stripe which extends along the step length L_y in a width d_{Debye} since there the capacitor has a larger thickness $d_{\mathrm{Debye}}+h$ when h is the step height. The line capacitance C_{step} can thus be estimated roughly as:

$$C_{step} = \boldsymbol{a}\boldsymbol{ee}_0\, d_{Debye}\left(\frac{1}{d_{Debye}+h} - \frac{1}{d_{Debye}}\right) \tag{14}$$

Here α is a fitting factor of the order of one. This line capacitance is again in series with the Helmholtz-capacitance in the same stripe area. After some trivial algebra one obtains for the total line capacitance

$$C_{step} = -\acute{a}\,\boldsymbol{ee}_0 \frac{h d_{Debye}}{(\acute{a}\, d_H + d_{Debye})(\acute{a}\, d_H + h + d_{Debye})} \tag{15}$$

in which d_{H} is

$$d_H = \frac{\boldsymbol{ee}_0}{C_H} \tag{16}$$

These equations only hold for small deviation of the potential from pzc, i. e. where the Gouy-Chapman capacitance has its minimum. For larger potential ϕ the effective screening length becomes shorter due to the non-linearity of the Poisson-Boltzmann equation. The effect of the non-linearity on the line capacitance will be studied later numerically. We note that the effect of a statistical roughness on the specific capacitance has been studied in quite some detail earlier by Daikhin et al. [23]. However, eq. (15) , cannot be recovered from this earlier work because of the rather different geometry of a step. Presumably a periodic array of steps such as on vicinal surfaces could be handled by the mathematical methods developed in [23]. However, we abstained from proceeding further along those lines because the numerical analysis is rather straightforward and, more importantly, we shall find the contribution from the step dipole moment to the line capacitance prevailing.

The dipole moment is due to the well known Smoluchowski effect [10]: Near a step the electron charge density contours follow the step contour but smoothly in order to save kinetic energy at the expense of building up the electrostatic energy associated with the local deviation from neutrality. The vertical component of the step dipole moment gives rise to a reduction in the work function on vicinal surfaces with regular step arrays and likewise to a lowering of pzc, and can therefore be measured for surfaces in vacuum [11] as well as in contact with an electrolyte [13]. Due to water adsorption the dipole moment measured in the two cases need not be the same. The relation between the vertical component of the dipole moment per step atom p_z and the reduction in the work function, respectively the lowering of pzc $\Delta \boldsymbol{F}$ is

$$p_z = \boldsymbol{e}_0 \, a_{||} \, L_{step} \; \text{Ä}\boldsymbol{F} \tag{17}$$

Here, $a_{||}$ is atom the diameter and L_{step} the distance between the steps. Eq. (17) can either be derived by a formal integration of the dipole potentials, or, straightforwardly by considering a homogeneous distribution of dipoles in the continuum limit. For our considerations here we are interested in the local variation of the potential due to the surface dipole of steps which are assumed to be straight and infinitely long. In the cartesian coordinates as defined above, one obtains for the electrostatic potential caused by the step dipole

$$\boldsymbol{j}_s(x, z) = \frac{1}{2\boldsymbol{pe}_0 a_{||}} \left(p_z \frac{z}{x^2 + z^2} + p_x \frac{x}{x^2 + z^2} \right) \tag{18}$$

with p_x the parallel component of the step dipole moment. Note that the calculation is for a point dipole and is with reference to the plane z = 0! The potential arising from the perpendicular dipole moment p_z to be added locally to the potential of the electrode is twice the amount. The electrostatic potential gives rise to a local variation in the double layer charge which effects the step capacitance as well as the step tension. Since the qualitative effect of the additional dipole potential on the step tension is easier to estimate than the effect on the capacitance we consider the effect on the step tension. The differential step tension is calculated from eq. (4) with the charge densities

$$s_0(f) = \int_0^{f} C_0(f')\,df' \qquad (19)$$

$$s_s(x,f) = \int_0^{f+2j_s(x,z)} C_s(x,f')\,df' \qquad (20)$$

Here C_s and C_0 are the surface capacitances with and without the presence of a step, respectively. The capacitance $C_s(\mathrm{x},f')$ can be approximated by (see discussion above)

$$C_s(\mathrm{x},f') = C_0(f') + \begin{cases} C_{step}/d_{Debye} & 0 < \mathrm{x} < d_{Debye} \\ 0 & \text{else} \end{cases} \qquad (21)$$

With this expression for the capacitance C_s the charge density $s_s(\mathrm{x},f)$ becomes:

$$s_s(\mathrm{x},f) = \int_0^{f} C_0(f')\,df' + \int_f^{f+2j_s(\mathrm{x,z})} C_0(f')\,df' + \begin{cases} C_{\mathrm{step}}/d_{\mathrm{Debye}}(f + 2j_s(\mathrm{x,z}) & 0 < \mathrm{x} < d_{Debye} \\ 0 & \text{else} \end{cases} \qquad (2$$

2)

With the further approximation $j_s << f$ and $C_{\mathrm{step}}(f) = C_{\mathrm{step}}(0)$ one obtains for the line tension

$$\mathrm{d}b(f) \approx -C_{\mathrm{step}}\,f\,\mathrm{d}f - C_0(f)\,\mathrm{d}f \int_{-\infty}^{+\infty} 2j_s(\mathrm{x},z)\mathrm{dx} \qquad (23)$$

The integral over φ_s (eq. (18)) is independent of z and one obtains for the line tension:

$$\beta(\phi) - \beta_0 = -\frac{p_z}{\varepsilon_0 \alpha_{\|}} \sigma_0(\phi) - \frac{1}{2} C_{\mathrm{step}} \phi^2 \tag{24}$$

The first term which arises from the dipole potential is roughly linear in ϕ, the second term is the normal term from the step capacitance due to the geometric structure of the step. Since the step capacitance is negative (eq. 15) the geometric structure of the step contributes always positively to the step tension.

4. The numerical solution of the Poisson-Boltzmann equation

The step capacitance and the contribution of the ionic space charge layer to the line tension of a step are determined by a numerical solution of the Poisson-Boltzmann equation in two dimensions with the step structure and the potential distribution at the step as the boundary condition. In an improved simulation the relevant geometric structure of the step should be the position of the image plane and the boundary condition for the potential should be the potential on the image plane. Here, the geometric structure of the boundary is modeled by a (100) oriented x, y plane with a (111) oriented step of height h. In order to make contact with the experimental work of Dieluweit et al. [8] all geometric parameters are taken as for the Au(100) surface. The potential distribution on this boundary is chosen as to be that of a point dipole. Hence, the boundary $z_{\mathrm{surf}}(x)$ near the step at x=0 bears the potential

$$\phi(\mathrm{x}, \mathrm{z}_{\mathrm{surf}}(\mathrm{x})) = \phi + \frac{p_z}{\pi \alpha_{\|} \varepsilon_0} \frac{h}{\mathrm{x}^2 + h^2} \tag{25}$$

We have tested the model for the potential by varying (i) the exact position of the dipole and (ii) by adding the potential of a parallel component of the dipole of the same magnitude as the perpendicular component (which contributes a negative potential to the lower step edge) and found that these modifications have merely a minor effect on the step line tension. A non-trivial problem in modeling the step are the inner Helmholtz-layer of immobile water molecules and the response of the metal surface charge to an external field at a step. For a flat surface the response of the surface charge to an external field has been treated in the jellium model [22]. For a step this issue will be addressed in a forthcoming publication [15]. For the moment, we describe the effect of the inner layer in the same way as it is frequently done for the flat surface, namely by giving the Helmholtz-layer a potential independent capacitance. In the particular case of a surface structured by a step the thickness of the layer needs to be specified. We assume the layer to have a constant thickness of 3 Å with a sharp boundary towards the solution. Since thickness and capacitance are chosen arbitrarily (though guided by experimental data) the dielectric constant of the layer (which follows from the assumed capacity and thickness as $\varepsilon_H = 20$) differs from the dielectric constant of water ($\varepsilon = 78$). This imposes additional boundary conditions at the interface between the Helmholtz-layer and the liquid electrolyte which are not automatically fulfilled in the standard algorithm for solving the Poisson-equation. As well known (see e.g. [24]), the Poisson-equation is solved by a repetitive use of the algorithm

$$\phi(\mathrm{i},\mathrm{j}) = \frac{1}{4}\left(\phi(\mathrm{i}-1,\mathrm{j}) + \phi(\mathrm{i}+1,\mathrm{j}) + \phi(\mathrm{i},\mathrm{j}-1) + \phi(\mathrm{i},\mathrm{j}+1) + \frac{\rho(\mathrm{i},\mathrm{j})}{\varepsilon\varepsilon_0}\right) \quad (25)$$

in which i, j denote points on a two-dimensional grid. The cartesian coordinates of each grid point (x, z) are given (iΔx, jΔz) with $\Delta x = \Delta z$ the length unit of the grid. The boundary conditions on the interface between the Helmholtz-layer and the electrolyte are fulfilled if on the boundary itself eq. (25) is replaced by (see Appendix A)

$$\phi(\mathrm{i},\mathrm{j}) = \frac{\varepsilon(\mathrm{i}-1,\mathrm{j})\phi(\mathrm{i}-1,\mathrm{j}) + \varepsilon(\mathrm{i}+1,\mathrm{j})\phi(\mathrm{i}+1,\mathrm{j}) + \varepsilon(\mathrm{i},\mathrm{j}-1)\phi(\mathrm{i},\mathrm{j}-1) + \varepsilon(\mathrm{i},\mathrm{j}+1)\phi(\mathrm{i},\mathrm{j}+1)}{\varepsilon(\mathrm{i}-1,\mathrm{j}) + \varepsilon(\mathrm{i}+1,\mathrm{j}) + \varepsilon(\mathrm{i},\mathrm{j}-1) + \varepsilon(\mathrm{i},\mathrm{j}+1)} \quad (26)$$

Using this algorithm, the surface charge distribution near a step, the step capacitance, and the step tension were calculated on a grid size of 200x300, for the x- and y-direction respectively. The metric of the system was set by assigning 20 pixels to the step height of h = 2.04 Å. The far most side boundaries of the grid in x-direction ($\phi(0,j)$ and $\phi(200,j)$) were loaded with the analytical solution of the Poisson-Boltzmann equation and kept fixed while the algorithm ran over the grid. In the presence of a Helmholtz-layer the solution of the Poisson-Boltzmann equation for a flat surface cannot be expressed in a single closed form since the potential ϕ_G at the interface between the Helmholtz-layer and the liquid electrolyte on the one hand is determined by the voltage division between the Helmholtz-capacitance and the Gouy-Chapmann capacitance (eq. (13)), while on the other hand the Gouy-Chapman capacitance is also a function of the potential ϕ_G (eq. (11)). A self-consistent solution is however easily calculated numerically. With these rigid boundary conditions a relatively large over-relaxation of 1.95 [24, 25] (stability limit is 2.0) could be used which ensured good convergence of the results after about 300 repetitions.

5. Results

In order to be able to separate conceptually between the effect of the step structure and the dipole potential at the step, calculations were performed with and without the dipole potential. The results for the calculations with the step dipole were found to be almost unaffected by the position of the center of the dipole potential. This is in accordance with the analytical model which shows that the main contribution to the line tension is from the product of the surface charge with the integral over the dipole potential (eq. (24)). Small corrections which are sensitive to the local position of the step dipole arise from the variation of the local capacitance near the step site. Whether or not the dipole moment has a significant effect on the line tension depends on the magnitude of the dipole moment. The dipole moment can be taken from independent experiments, either from the variation of the work function with the step density on crystals or by the variation of the potential of zero charge with the step density. The variation of pzc on gold surfaces has been studied by Lecoeur et al. [26] for a large number of vicinal surfaces. For Au(111) vicinals, the pzc-data yield a dipole moment of $p_z = 0.04$ eÅ and $p_z = 0.06$ eÅ for the (100) and the (111) steps respectively. The results agree with the work function measurements within about 30% [11]. The difference is attributed to the dipole moment of the adsorbed water molecules [26]. The data of Lecoeur et al. include also the Au(1,1,19) surface which consists of (100) terraces with (111) step every 9.5 atom distances. For this surface the step dipole moment is calculated to be $p_z = 0.013$ eÅ. Recent theoretical calculations on the same surface in contact with a model electrolyte [27] are also in rough agreement with experimental data. We note that the step dipole seems to be particular large on Au(111). On Ag(111) one calculates a dipole moment of $p_z = 0.021$ eÅ for the B-steps from the variation of pzc [14].

We consider the results of the simulations without a step dipole first. The results are calculated for a fixed and potential independent Helmholtz-capacitance of 60 μF/cm^2. The Debye length d_{Debye} is varied between 9 Å and 30 Å (which corresponds to concentrations of monovalent electrolytes between 0.1 M and 0.01 M). Fig. 2 displays the (differential) surface and step capacitances. The surface capacitance is here calculated with the simulation program, but is equivalent to the results of the standard Gouy-Chapman theory with a Helmholtz-layer. The surface capacitance shows the characteristic minimum at pzc which is often used to determine the potential of zero charge experimentally. For larger deviations from pzc the Gouy-Chapman capacitance becomes very large (eq. (11)). The total capacitance therefore approaches the capacitance of the Helmholtz-layer (eq. (13)). The potential dependence of the line capacitance displays several interesting feature. For large deviations from pzc the line capacitance is very small, independent of the Debye-length. For large potentials the decay length of the space charge becomes very small. As a consequence the equi-potential lines follow the geometric contour of the step (Fig. 2). The surface charge is then that of a flat surface. The total charge is however slightly larger because of the increased surface area due to the step contour. At pzc the line capacitance displays a maximum for larger d_{Debye} and a minimum for small d_{Debye}. Again this result is easily understood by considering the equi-potential lines. At pzc and for large d_{Debye} the equi-potential lines follow the geometric step contour only smoothly, so that the lower edge of the step is effectively screened which results in a negative line capacitance (see discussion in sect. 3). As the potential increases the screened range near the step stays approximately constant until for larger potentials most of the potential drop in the Gouy-Chapman layer is within a distance of the order of a step height. Since the Gouy-Chapman capacitance increases the absolute value of the line capacitance also increases, until eventually the equi-potential lines follow the step contour closely as described above. The latter effect takes over immediately even for smaller potentials when the Debye-length is short. The surface tension according to the Gouy-Chapman theory and as calculated here and the line tension for steps without a step dipole are presented in Fig. 4. Since the line capacitance is negative, the line tension is positive for all potentials. The absolute numbers are, however, rather small compared to typical step energies which are of the order of 100 meV. Fig. 5 shows the dependence of the line capacitance at pzc on the Debye-length. The full line is a fit to eq. (15) with $\alpha = 0.29$. The agreement between the analytical model and the numerical simulations is quite pleasing.

We now consider the effect of the step dipole. As for the magnitude of the dipole moment we choose a value of $p_z = 0.015$ eÅ which is approximately the dipole moment of steps on Au(100) [26]. With the step-dipole, the line capacitance is dramatically larger and assumes an S-shaped function of the potential (Fig. 6). Likewise is the line tension considerably larger and approximately a linear function of the potential (Fig. 7). Although the calculations include the geometric effect on the line capacitance the tension is completely dominated by the dipole contribution. The line tension depends little on the Debye-length of the electrolyte. The approximate linearity of the dependence on the potential, the absolute magnitude, and the small effect of the Debye-length are in agreement with the model developed in sect. 3. According to eq. (24) the line tension should be proportional to the dipole moment and the surface charge of the step free surface. In Fig. 8 the result of the simulation is compared with eq. (24), with the surface charge calculated from the Gouy-Chapman theory (with the constant Helmholtz-capacitance of 60 µF/cm^2). The agreement is again quite acceptable considering the approximations in the model. We conclude therefore that the potential dependence of the step line tension in the absence of specific adsorption can be quite approximated by

$$b(f) = b(f_{\mathrm{pzc}}) - \frac{p_z}{e_0 a_{\|}} s_0(f) \quad . \qquad (27)$$

We note that the capacitance of the Helmholtz-layer need not be potential independent for eq. (27) to hold since any variation of the Helmholtz-capacitance leads to a variation in the dependence of the surface charge on the potential and is taken care of in the formulation of eq. (27). With this remarkable equation at hand, one is now in a position to calculate the potential dependence of the step line tension from data obtained in conventional electrochemical experiments. The surface charge as a function of the potential is obtained from integrating voltamograms and the dipole moment can be calculated from the shift of the pzc on vicinal surfaces (eq. 17).

6. Discussion

Although the results presented in this paper are based on a model for the true potential at steps there are several salient features which should persist in a rigorous theory of the complete solid/electrolyte interface. As we have seen, the by far largest contribution of the space charge region of mobile ions to the step line tension results from the reduced work function near steps which is a consequence of the dipole moment associated with the charge distribution at steps. The comparison of the change in the work function in vacuum and the variation of pzc for Au(100) [11, 13, 26] shows that the step dipole moment is not dramatically affected by the presence of an electrolyte (in the absence of specific adsorption at steps, that is!). The contribution of the step dipole moment to the interfacial line tension which arises from the space charge continuum of mobile ions should therefore be also independent on the microscopic details of the solid/electrolyte interface and the electrolyte composition, if the effect is expressed in terms of the specific surface charge and if there is no specific adsorption of ions. Fig. 8 shows that the semi-macroscopic contribution to the line tension of steps is nearly a linear function of the surface charge, and therefore a smooth function of the surface potential, with a decreasing line tension for positive potentials. Neither the smooth dependence nor the overall decrease of the line tension is in agreement with the so far only experiment on the dependence of the step line tension as a function of the potential on the Au(100) surface in sulfuric acid [8]. It is however well known that SO_4^--ions are specifically adsorbed on gold surfaces [28-30]. Specific adsorption necessarily modifies the potential dependence of the line tension. Specific adsorption at step sites changes the dipole moment. The step excess also enters directly via the thermodynamics (eq. (4)). A potential dependent excess adsorption is therefore directly reflected in the line tension of steps. The experimentally observed sharp features in the step line tension as a function of potential in [8] are therefore attributed to specific adsorption.

The considerations in this paper concerning the role of step dipoles on the step line tension can be carried over to the dependence of the energy of other defects on the potential. Kinks in steps, e. g., are expected to carry an even larger dipole moment than steps because of the more open structure. Hence, the kink energy should decrease with positive potentials, just as the step line tension. The same can be said about the (Gibbs) free energy (to be defined again under conditions of constant electrode potential, not constant charge) of a single atom on a terrace. The reduction of the kink energy for positive potentials would lead to an increase in the mass transport along steps and thereby to larger step fluctuations for positive potential. The decrease of the effective activation energy should be approximately proportional to the line charge, and hence approximately proportional to the electrode potential, at least in a small potential range. This behavior has indeed been observed [31-33]. Again the effect of the surface charge on the activation energies as calculated in the EAM-model would contribute as an additional effect [27].

We finally comment that the contribution of the step dipole moment to the step line tension may have interesting consequences for step-step interactions at close distance. The dipole moment of steps at close proximity should be distance dependent, and hence the total energy should likewise become a function of the step distance. At present no theoretical calculations on the magnitude of the dipole moment as a function of step distance are available. Hence, nothing can be said about the magnitude of the effect.

Acknowledgements

This work was supported by the Fond der Chemischen Industrie which is gratefully acknowledged. The authors acknowledge furthermore helpful discussions with A. Liebsch.

Appendix A

The scenario considered in this paper requires the self-consistent solution of the Poisson-Boltzmann equation for the liquid together with the Laplace equation for Helmholtz layer, with a nontrivial boundary between the two media. Thus, the algorithm must ensure the fulfillment of the boundary condition that the parallel and perpendicular component of the electric field and displacement are continuous at the boundary, respectively. To develop the algorithm we first need to define the boundary grid points: we introduce a height function $z_H(i)$ which describes the boundary of the Helmholtz layer at each column i (black filled points in Fig. A1). The function can be made to fulfill the condition $z_H(x_i) \geq z_H(x_{i+1})$ so that the points (i, j) with $z_H(x_{i+1}) \leq \Delta j \leq z_H(x_i)$ are points on the boundary (gray filled points in Fig. A1) and constitute a vertical section on the boundary if $z_H(x_i) - z_H(x_{i+1}) \geq 2\Delta z$. All grid points below and to the left of the boundary and the points on the boundary (filled and open circles in Fig. A1) belong to the Helmholtz layer with a dielectric constant $e(i, j) = e_H$ (= 20 e.g.), and the points above and on the right of the boundary belong to the electrolyte with a dielectric constant $\varepsilon(i, j) = \varepsilon_G$ (= 78) and a non-vanishing space charge $\rho(i, j)$. The boundary conditions are fulfilled if on the boundary (i, j)

$$e(i+1, j)\frac{\partial f}{\partial x}\bigg|_{i+0} - e(i-1, j)\frac{\partial f}{\partial x}\bigg|_{i-0} + e(i, j+1)\frac{\partial f}{\partial z}\bigg|_{j+0} - e(i, j-1)\frac{\partial f}{\partial z}\bigg|_{j-0} = 0 \qquad \text{(A1)}$$

Here the symbols i ±0 and j ±0 denote that the derivatives are taken on a point infinitesimally shifted away from the exact position. For a point (i, j) on a horizontal boundary one has $e(i-1,j) = e(i,j) = \varepsilon(i+1,j) = e(i,j-1) = e_H$, and $e(i,j+1) = e_G$ so that

$$e_H\frac{\partial f}{\partial x}\bigg|_{i+0} - e_H\frac{\partial f}{\partial x}\bigg|_{i-0} + e_G\frac{\partial f}{\partial z}\bigg|_{j+0} - e_H\frac{\partial f}{\partial z}\bigg|_{j-0} = 0 \qquad \text{(A2)}$$

Eq.(A2) is fulfilled if

$$\left.\frac{\partial f}{\partial \mathrm{x}}\right|_{\mathrm{i+0,j}} = \left.\frac{\partial f}{\partial \mathrm{x}}\right|_{\mathrm{i-0,j}} \qquad\qquad \text{(A3)}$$
$$e_G \left.\frac{\partial f}{\partial \mathrm{z}}\right|_{\mathrm{i,j+1}} = e_H \left.\frac{\partial f}{\partial \mathrm{z}}\right|_{\mathrm{i,j-1}}$$

which are just the required boundary conditions. In the same way it can be shown that the boundary conditions are obeyed on a vertical interface if eq. (A1) holds. The algorithm which secures eq. (A1) is derived analogous to the derivation of the standard algorithm for the solution of the Laplace-equation. On the interface one has the Taylor-expansions of ϕ(i, j)

$$\begin{aligned}
f(\mathrm{i}-1,\mathrm{j}) &= f(\mathrm{i},\mathrm{j}) - \left.\frac{\partial f}{\partial \mathrm{x}}\right|_{\mathrm{i-0}} \Delta\mathrm{x} + \frac{1}{2}\left.\frac{\partial^2 f}{\partial \mathrm{x}^2}\right|_{\mathrm{i-0}} \Delta\mathrm{x}^2 \\
f(\mathrm{i}+1,\mathrm{j}) &= f(\mathrm{i},\mathrm{j}) + \left.\frac{\partial f}{\partial \mathrm{x}}\right|_{\mathrm{i+0}} \Delta\mathrm{x} + \frac{1}{2}\left.\frac{\partial^2 f}{\partial \mathrm{x}^2}\right|_{\mathrm{i+0}} \Delta\mathrm{x}^2 \\
f(\mathrm{i},\mathrm{j}-1) &= f(\mathrm{i},\mathrm{j}) - \left.\frac{\partial f}{\partial \mathrm{z}}\right|_{\mathrm{j-0}} \Delta\mathrm{z} + \frac{1}{2}\left.\frac{\partial^2 f}{\partial \mathrm{z}^2}\right|_{\mathrm{j-0}} \Delta\mathrm{z}^2 \\
f(\mathrm{i},\mathrm{j}+1) &= f(\mathrm{i},\mathrm{j}) + \left.\frac{\partial f}{\partial \mathrm{z}}\right|_{\mathrm{j+0}} \Delta\mathrm{z} + \frac{1}{2}\left.\frac{\partial^2 f}{\partial \mathrm{z}^2}\right|_{\mathrm{j+0}} \Delta\mathrm{z}^2
\end{aligned} \qquad \text{(A4)}$$

By multiplying the four expansions with e(i-1,j), e(i+1,j), e(i,j-1), and e(i,j+1), respectively and after summing one obtains with Δx = Δz

$$\begin{aligned}
&e(\mathrm{i}-1,\mathrm{j})\,f(\mathrm{i}-1,\mathrm{j}) + e(\mathrm{i}+1,\mathrm{j})\,f(\mathrm{i}+1,\mathrm{j}) + e(\mathrm{i},\mathrm{j}-1)\,f(\mathrm{i},\mathrm{j}-1) + e(\mathrm{i},\mathrm{j}+1)\,f(\mathrm{i},\mathrm{j}+1) \\
&= \left[e(\mathrm{i}-1,\mathrm{j}) + e(\mathrm{i}+1,\mathrm{j}) + e(\mathrm{i},\mathrm{j}-1) + e(\mathrm{i},\mathrm{j}+1)\right] f(\mathrm{i},\mathrm{j})
\end{aligned} \qquad \text{(A5)}$$

if eq. (A1) and the Laplace-equation $\frac{\partial^2 f}{\partial \mathrm{x}^2} + \frac{\partial^2 f}{\partial \mathrm{z}^2} = 0$ is obeyed. Eq. (A5) is the required algorithm.

References

[1] H.-C. Jeong, E. D. Williams, Surf. Sci. Rep. 34 (1999) 171.

[2] M. Giesen, Prog. Surf. Sci. 68 (2001) 1.

[3] G. Schulze-Icking-Konert, M. Giesen, H. Ibach, Phys. Rev. Lett. 83 (1999) 3880.

[4] M. Giesen, C. Steimer, H. Ibach, Surf. Sci. 471 (2001) 80.

[5] D. C. Schlößer, L. K. Verheij, G. Rosenfeld, G. Comsa, Phys. Rev. Lett. 82 (1999) 3843.

[6] C. Steimer, M. Giesen, L. Verheij, H. Ibach, Phys. Rev. B 64 (2001) 085416.

[7] S. Baier, S. Dieluweit, M. Giesen, Surf. Sci. 502/503 (2002) 463.

[8] S. Dieluweit, H. Ibach, M. Giesen, Trans. Farad. Soc. 121 (2002) in press.

[9] S. Dieluweit, M. Giesen, J. Phys.:Cond. Mat. in press (2002).

[10] R. Smoluchowski, Phys. Rev. 60 (1941) 661.

[11] K. Besocke, B. Krahl-Urban, H. Wagner, Surf. Sci. 68 (1977) 39.

[12] J. F. Jia, K. Inoue, Y. Hasegawa, W. S. Yang, T. Sakurai, Phys. Rev. B 58 (1998) 1193.

[13] A. Hamelin, in B. E. Conway, R. E. White, J. O. M. Bockris (Eds.): *Modern Aspects of Electrochemistry, Vol. 16*, Plenum, New York

London 1985.

[14] A. Hamelin, L. Stoicoveciu, L. Doubova, S. Trasatti, Surf. Sci. 201 (1988) L498.

[15] H. Ibach, W. Schmickler, to be published (2003).

[16] W. Schmickler, *Interfacial Electrochemistry*, Oxford University Press, Oxford 1995.

[17] W. Schmickler, E. Leiva, J. Electroanal. Chem. 453 (1998) 61.

[18] J. Richev, J. Lipkowski, J. Electrochem. Soc. 133 (1986) 121.

[19] J. Lipkowski, W. Schmickler, D. M. Kolb, R. Parsons, J. Electr. Anal. Chem. 452 (1998) 193.

[20] G. Gouy, J. Phys. (Paris) 9 (1910) 457.

[21] D. L. Chapman, Philos. Mag. 25 (1913) 475.

[22] W. Schmickler, D. Henderson, Progr. Surf. Sci. 22 (1986) 232.

[23] L. I. Daikhin, A. A. Kornyshev, M. Urbakh, Phys. Rev. E 53 (1996) 6192.

[24] H. Ibach, *Electron Energy Loss Spectroscopy - The Technology of High Performance*, Springer-Verlag, Heidelberg 1991.

[25] E. W. Schmid, G. Spitz, W. Lösch, *Theoretische Physik mit dem Computer*, Springer, Berlin, Heidelberg 1987.

[26] J. Lecoeur, J. Andro, R. Parsons, Surf. Sci. 114 (1982) 320.

[27] M. I. Haftel, T. L. Einstein, Appl. Surf. Sci. 175/176 (2001) 49.

[28] Z. Shi, J. Lipkowski, M. Gamboa, P. Zelenay, A. Wieckowski, J. Electroanal. Chem 366 (1994) 317.

[29] Z. Shi, J. Lipkowski, S. Mirwald, B. Pettinger, J. Electroanal. Chem. 396 (1995) 115.

[30] I. R. d. Moraes, F. C. Nart, J. Electroanal. Chem. 461 (1999) 110.

[31] M. Giesen, M. Dietterle, D. Stapel, H. Ibach, D. M. Kolb, Proc. Mat Res. Soc. 451 (1997) 9.

[32] M. Giesen, M. Dietterle, D. Stapel, H. Ibach, D. M. Kolb, Surf. Sci. 384 (1997) 168.

[33] M. Giesen, R. Randler, S. Baier, H. Ibach, D. M. Kolb, Electrochim. Acta 45 (1999) 527.

Figure Captions

Fig. 1: Equipotential contours at a step for a step height h = 2 Å, a Debye-length of d_{Debye} = 10 Å and an electrode potential of 0.05 V vs. pzc. No Stern layer of specifically adsorbed ions is assumed. Since the potential contours at the vertical distance d_{Debye} follow the step contour but smoothly over a lateral distance which is again approximately d_{Debye}, the effective capacitance is reduced near the step.

Fig. 2: Surface and line capacitance (without a step dipole) for an assumed Helmholtz-capacitance of 60 $\mu F/cm^2$ as a function of the potential and the Debye-length. The line capacitance of a step depends on the details of the assumed step geometry.

Fig. 3: Equi-potential lines near a step with an inner Helmholtz-layer of 3 Å thickness. The Debye-length of the electrolyte is 30 Å. The equi-potential lines are densely spaced inside the Helmholtz-layer, because of the high capacity of that layer. Fig. 3 (a) and (b) are for electrode potentials of 1 V and 20 mV, respectively.

Fig. 4: Surface and line tension in the absence of a step dipole.

Fig. 5: Numerical calculation of the line capacitance at pzc compared to the analytical expression (eq. (15)).

Fig. 6: Surface and line capacitance for a step with a step dipole of p_z = 0.015 eÅ.

Fig. 7: Surface and line tension for a step with a step dipole of p_z = 0.015 eÅ.

Fig.8: Line tension of a step with a step dipole of p_z = 0.015 eÅ plotted vs. the surface charge density σ_0. The full line represents the analytical model (eq. (24)).

Figures

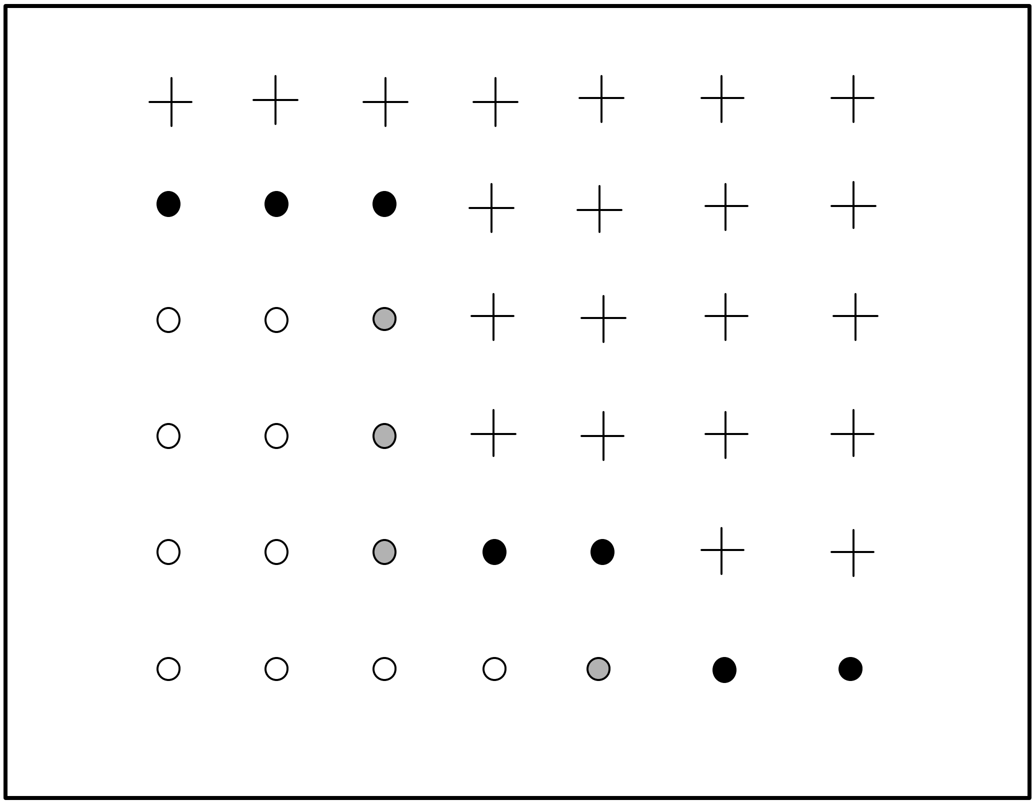

Fig. A1

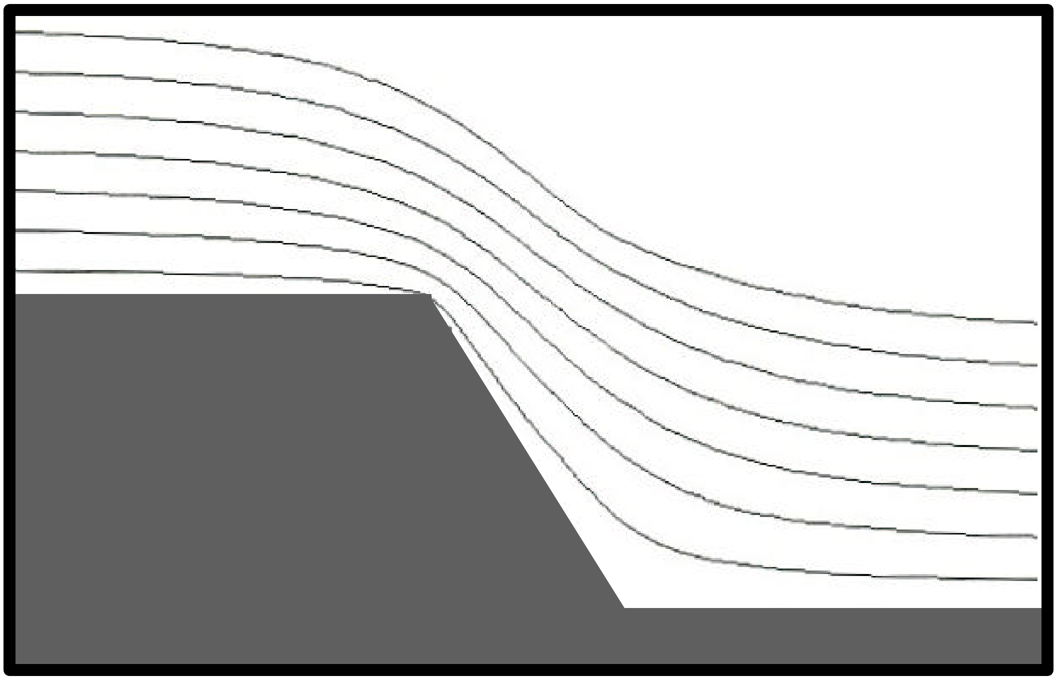

Fig.1

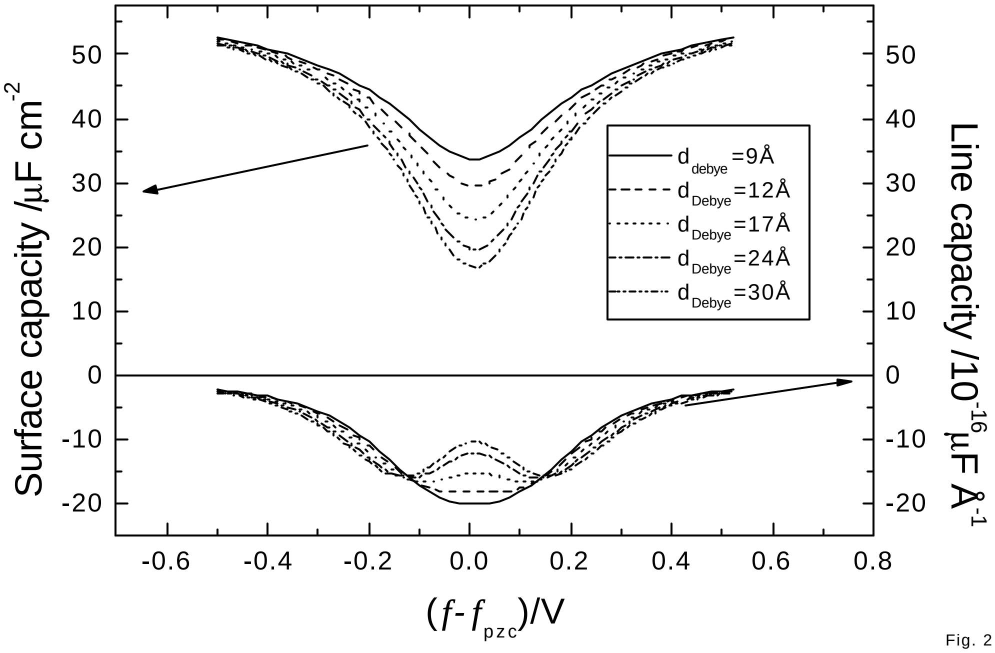

Surface capacity /µF cm^{-2}
Line capacity /10^{-16} µF Å^{-1}
(f- f$_{pzc}$)/V
d$_{debye}$=9Å
d$_{Debye}$=12Å
d$_{Debye}$=17Å
d$_{Debye}$=24Å
d$_{Debye}$=30Å
50
40
30
20
10
0
-10
-20
-0.6
-0.4
-0.2
0.0
0.2
0.4
0.6
0.8

Fig. 2

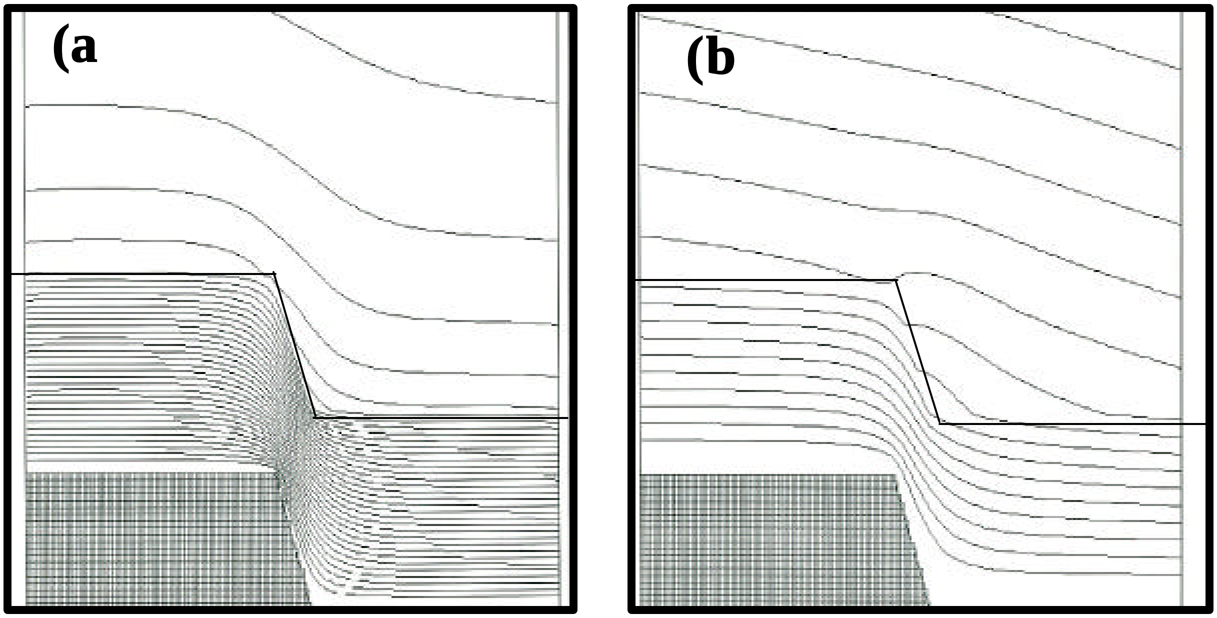
(a
(b

Fig. 3 3

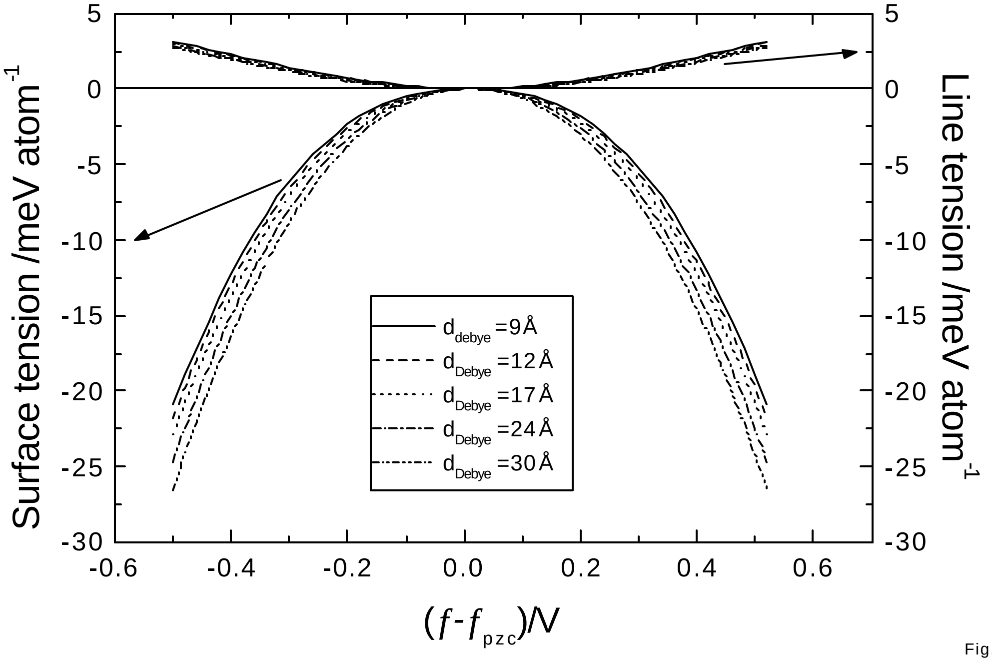
Surface tension /meV atom^{-1}
Line tension /meV atom^{-1}
$(f-f_{pzc})/V$
5
0
-5
-10
-15
-20
-25
-30
-0.6
-0.4
-0.2
0.0
0.2
0.4
0.6
d_{debye} =9Å
d_{Debye} =12Å
d_{Debye} =17Å
d_{Debye} =24Å
d_{Debye} =30Å

Fig. 4

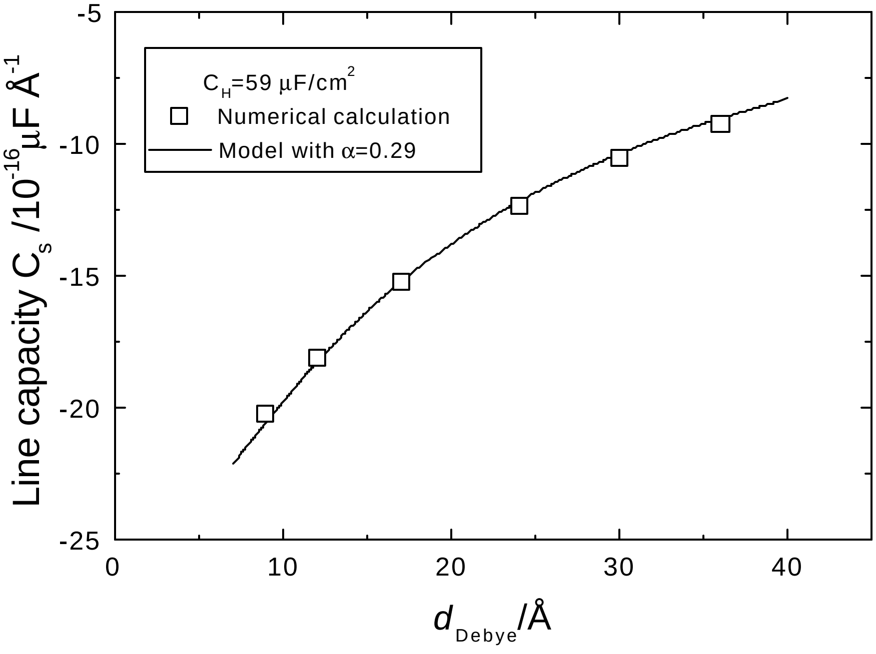
-5
-10
-15
-20
-25
0
10
20
30
40
Line capacity C_s /10^-16 µF Å^-1
d_Debye/Å
C_H=59 µF/cm^2
Numerical calculation
Model with α=0.29

Fig. 5

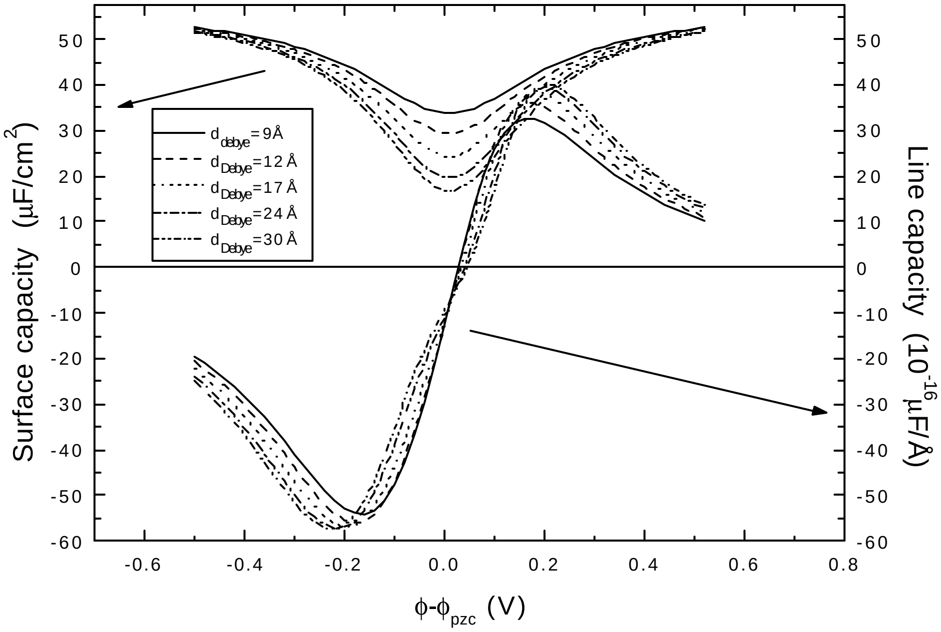
50
40
30
20
10
0
-10
-20
-30
-40
-50
-60
-0.6
-0.4
-0.2
0.0
0.2
0.4
0.6
0.8
Surface capacity (µF/cm^2)
Line capacity (10^-16 µF/Å)
φ-φ_pzc (V)
d_debye=9Å
d_Debye=12 Å
d_Debye=17 Å
d_Debye=24 Å
d_Debye=30 Å

Fig. 6

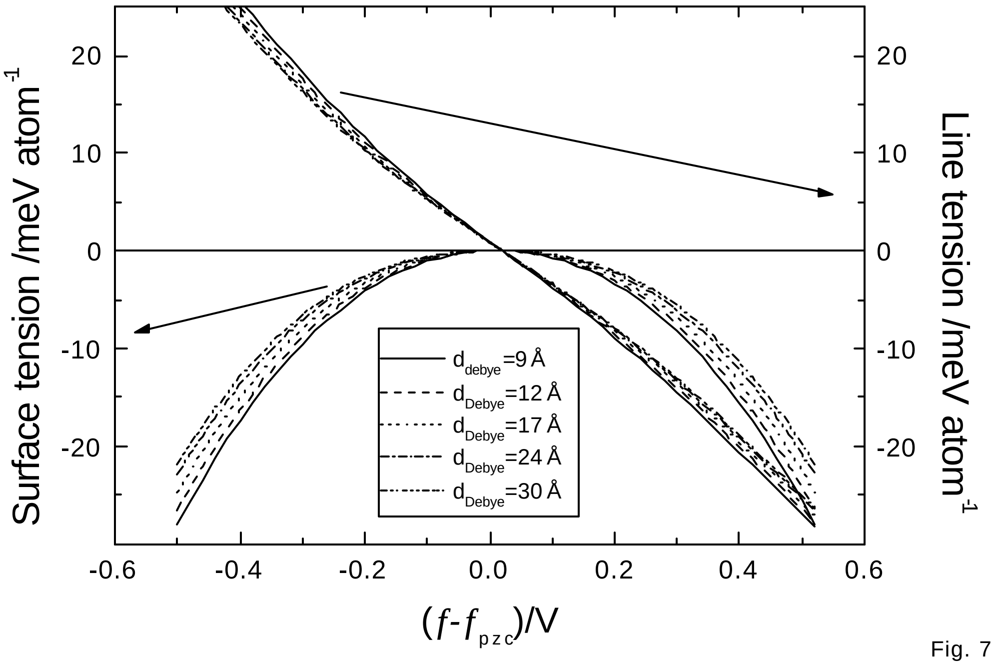
Surface tension /meV atom^{-1}
Line tension /meV atom^{-1}
$(f-f_{pzc})$/V
20
10
0
-10
-20
-0.6
-0.4
-0.2
0.0
0.2
0.4
0.6
d_{debye}=9 Å
d_{Debye}=12 Å
d_{Debye}=17 Å
d_{Debye}=24 Å
d_{Debye}=30 Å

Fig. 7

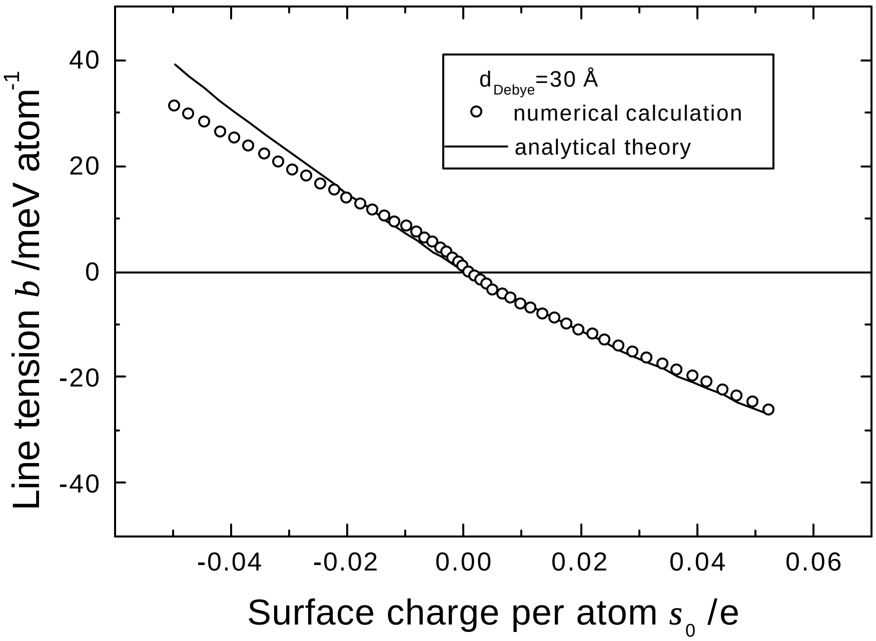
Line tension b /meV atom^{-1}
Surface charge per atom s_0 /e
40
20
0
-20
-40
-0.04
-0.02
0.00
0.02
0.04
0.06
d_{Debye}=30 Å
numerical calculation
analytical theory

Fig. 8